Article:

Audu, GA, Bhattacharya, S, Muhtar, A et al. (2 more authors) (2017) Reliability and quality of service of an off-grid wind powered roadside unit in a motorway vehicular environment. Vehicular Communications, 9. pp. 176-187. ISSN 2214-2096

https://doi.org/10.1016/j.vehcom.2017.07.001

Accepted Manuscript

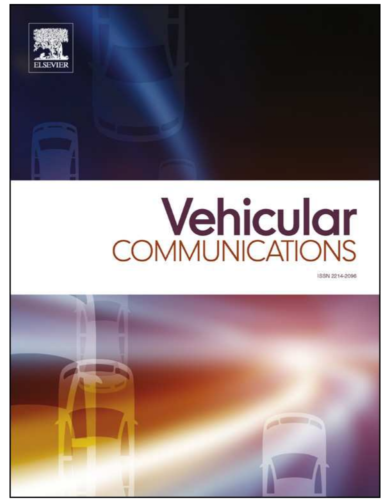

Reliability and quality of service of an off-grid wind powered roadside unit in a motorway vehicular environment

George A. Audu, Samya Bhattacharya, Adnan Muhtar, Bilal Qazi, Jaafar M.H. Elmirghani

PII: S2214-2096(16)30175-9
DOI: http://dx.doi.org/10.1016/j.vehcom.2017.07.001
Reference: VEHCOM 100

To appear in: *Vehicular Communications*

Received date: 28 November 2016
Revised date: 26 May 2017
Accepted date: 5 July 2017

Please cite this article in press as: G.A. Audu et al., Reliability and quality of service of an off-grid wind powered roadside unit in a motorway vehicular environment, *Veh. Commun.* (2017), http://dx.doi.org/10.1016/j.vehcom.2017.07.001

Reliability and Quality of Service of an Off-Grid Wind Powered Roadside Unit in a Motorway Vehicular Environment

George A. Audu, Samya Bhattacharya, Adnan Muhtar, Bilal Qazi, Jaafar M. H. Elmirghani

{elgaa,s.bhattacharya}@leeds.ac.uk, adnanmuhtar@hotmail.com, bilalqazipk@gmail.com, J.M.H.Elmirghani@leeds.ac.uk}

School of Electronic and Electrical Engineering, University of Leeds, UK

Abstract- Wind-powered base stations and roadside units have been considered as a cost effective greening solution in windy countries which also have limited solar irradiation. The practicality of such a system increases significantly in sparse areas such as countryside and motorways. The deployment of standalone off-grid wind powered roadside units could alleviate the common issues related to grid connected renewable energy farms. Hence, there is need to study the feasibility of an off-grid wind powered roadside unit for seamless connectivity. Unlike the conventional usage of reliability analysis of fault-tolerant systems, in this paper, reliability is redefined in the context of availability of intermittent wind for powering a roadside unit (RSU) in a UK motorway vehicular environment. Transient analysis of energy consumption (energy demand) of the RSU and harnessed wind energy are carried out along with real measurements for developing respective generic energy models. Further, a generalised methodology is developed to determine the minimum battery size for achieving a certain reliability standard and quality of service. Several reliability indices such as loss of load probability (LOLP), loss of load expectation (LOLE), energy index of reliability (EIR), mean time between failures (MTBF), mean time to recovery (MTTR), forced outage rate (FOR), etc. are obtained for the RSU. The performance results reveal that with a standard micro-turbine and a reasonably small battery, an RSU achieves a good reliability of 99.9% with significant improvement in the quality of service.

Keywords

Roadside unit; wind energy; reliability indices; motorway environment; vehicular network.

List of Abbreviations

AIR	Air information resource
AP	Access Point
BS	Base Station
CDF	Cumulative Distribution Function
DOD	Depth of Discharge
EENS	Expected Energy Not Supplied
EDNS	Expected Demand Not Served
EIR	Energy Index of Reliability
ELCC	Effective Load Carrying Capacity
FOR	Forced Outage Rate
ICT	Information and Communication Technology
LOEE	Loss of Energy Expectation
LOLE	Loss of Load Expectation
LOLP	Loss of Load Probability
MTBF	Mean Time before Failure
MTTF	Mean Time to Failure
MTTR	Mean Time to Repair
MW	Mega Watts
PDF	Probability Density Function
QoS	Quality of Service
RSU	Road Side Unit
SAPS	Small Autonomous Power Systems
SSWECS	Small Standalone Wind Energy Conversion Systems
V2R	Vehicle-to-Roadside
WAVE	Wireless Access in Vehicular Environments

List of Symbols

A	Cross-sectional area of wind turbine
C	Energy level of battery
D	Diameter of wind turbine
M	Vehicular density/ No of vehicles
W	Average packet delay
t	Time duration
v	Instantaneous wind speed
α	Scale parameter of Weibull distribution (for wind speed)
β	Shape parameter of Weibull distribution (for wind speed)
λ	Packet arrival rate
μ	Packet service rate
μ	Mean of Normal distribution
ρ	Air density

σ	Standard deviation of Normal distributed traffic load
C_p	Coefficient of performance
E_0	Energy demand of the system in a year
E_w	Wind Energy
P_{MAX}	Maximum operational power
P_{Idle}	Minimum operational power
P_s	Average packet size
P_t	Transmit power
P_w	Wind power
X_t	Throughput at hour t
$\bar{v}$	Mean wind speed
v_{cut-in}	Cut in speed for wind turbine
$v_{cut-off}$	Cut off speed for wind turbine
d_r	Data rate
d_t	Vehicle data generation rate
e_b	Energy per bit
α'	Scale parameter of Weibull distribution (for wind power)
β'	Shape parameter of Weibull distribution (for wind power)
E_{ns}	Expected demand not served
F_r	Forced outage rate
L_{lp}	Loss of load probability
L_{le}	Loss of load expectation
L_{ee}	Loss of energy expectation
T_{bf}	Time before failure
T_{tr}	Time to recovery/repair
U_d	Unmet demand

1. INTRODUCTION

The rising trends of 'connected vehicles' in the market, the rapid increase of motorway and urban road networks, and the need to deploy ubiquitous communications network among large number of vehicles (i.e. 34.6 million vehicles in the UK in 2012 [1]) suggest an imminent growth of vehicular networks comparable to that of the current cellular networks [2]. It is therefore evident that some of the existing operational challenges of cellular topology will be inherited in vehicular networks in addition to the challenge of maintaining seamless connectivity in highly mobile vehicles. Deployment of incumbent mobile technology to support vehicular communications is impractical considering the acute spectrum shortage which restrains higher data rates transmission and the associated large power consumption of complex base stations (BSs). Given that the emergence of vehicular communication networks is at a time the existing communication technologies are already consuming significant amounts of energy, and environmental concerns are rife, the key design objective of future vehicular networks should mitigate the problem of low data rates with the use of roadside units (RSUs) in a micro-macro topology. This may however be at the expense of potentially higher overall energy consumption [2].

Deployment of RSUs with renewable energy sources can significantly reduce the carbon footprint while standalone off-grid wind powered RSUs can as well alleviate common issues associated with grid connected renewable energy farms, and provide ease of operation (deployment and maintenance) in remote areas such as countryside and motorways. Such deployments also eliminate several power systems related issues such as distribution, metering and grid maintenance. With the renewable power generation technologies becoming increasingly cost-competitive and the option of off-grid electrification in most areas and locations with good resources becomes most economic [3], the renewable energy sources in conjunction with fast rechargeable batteries have become an attractive option to power the BSs/RSUs in sparse vehicular environments.

Since achievable renewable energy varies greatly based on the geographic locations and weather conditions, the design of reliable communication systems powered by renewable energy introduces additional complexity, especially in the case of standalone off-grid systems. Wind powered off-grid BSs/RSUs is a better option in windy countries like the UK, where the solar power is limited in several geographic locations for a substantial period of the year. The previous studies by the authors in [4][5] investigated the feasibility of a standalone wind-powered RSU in the UK and have shown that the communication Quality of Service (QoS) requirements can be met with a very small battery if a sleep mechanism is employed. In the related dissertation [5], reliability study of wind energy powered RSUs in a motorway environment was introduced and various power engineering reliability indices in the context of adequacy or inadequacy of the available wind energy were defined to meet the RSU load demand. The author, however, only obtained simulation results for the studied reliability indices such as LOLP, LOLE, EDNS, MTBF, MTTR and FOR without any analytic model. The study by the author was also limited to a single location (Reading in the UK) without any extension to and comparison with other geographic locations.

The work in this paper provides comprehensive models for the wind energy and RSU energy consumption and use them to develop analytic models for the various reliability indices. Other geographic locations with different climates are also studied and compared with the chosen location in the UK. Furthermore, queueing models of the studied RSU are developed to obtain some essential QoS metrics such as average packet delay and throughput in term of reliability index LOLP.

Our contributions in this paper are fourfold: (1) A transient analysis of energy consumption (energy demand) of the RSU based upon real vehicular traffic measurements has been carried out to develop a generic energy consumption model; (2) A transient analysis of harnessed wind energy based on the output of a micro-turbine and measured wind speed for the same geographic location has been carried out to develop a generic wind energy model; (3) Key reliability indices are redefined in the context of availability of intermittent wind power unlike the conventional usage of reliability analysis of fault-tolerant systems; and (4) corresponding analytic models have been proposed.

The rest of the paper is organised as follows: A brief discussion on related work is presented in Section II while Section III describes the studied scenario along with energy and communication parameters. Section IV details the wind energy model. Section V presents the energy consumption model of a standalone off-grid wind powered RSU. Section VI redefines and models the reliability indices for V2R scenario. The performance of the RSU in the context of reliability and QoS is analysed in Section VII, followed by the conclusion in Section VIII.

2. Related Work

The exponential growth in the cellular networks operators' market and the number of subscribers has increased cellular traffic. This invariably pushes the limits of energy consumption in wireless networks to adversely impact the industry's overall carbon footprint. The average annual energy consumption of a 3G BS is about 4.5 MWh with a typical 3G BS using about 500 W of input power to produce about 40 W of output RF power [5]. According to [6], 4G macro Long-Term Evolution (LTE) BS consumes no lesser power, having a power consumption of 1350 W at full load. Currently, BSs account for 57% of mobile operator's total energy expenditure [5]. With the current number of 3G and 4G base stations in the UK exceeding 12000 [5], about 50 GWh is spent in a year. This invariably leads to not only significant carbon emissions but also much higher operating costs for telecoms providers. In terms of the global carbon emissions, it is reported that information and communication technology (ICT) accounts for 2–2.5% of all harmful emissions [7]. According to [8], approximately 3% or 600 TWh of the worldwide electrical energy is consumed by the ICT sector, and it is estimated that energy consumption for ICT will grow to 1,700 TWh by 2030 [8].

Recent rapid advances in cellular technology has brought significant improvements and enhanced performance of mobile devices with high data consuming applications. The advent of android and iPhone devices alongside the massive penetration of social networking giants such as Facebook has necessitated high demand for data traffic and corresponding high operational energy in recent years. The inevitability of these challenges has compelled researchers and the industry to explore new technologies and strategies which are not only able to meet the unprecedented bandwidth and connectivity demand, but are also energy efficient. The use of renewable sources of energy such as wind or solar power proves to be an economic and attractive option that gives these devices complete independence [4]. Global environmental concerns associated with conventional energy generation have led to increase in the development of renewable alternative energy sources in power systems.

Many nations across the globe have set high wind penetration targets in their energy generation mix to mitigate the greenhouse effect arising from the conventional generations. A recent report from Pike Research, a part of Navigant's Energy Practice, states that the annual deployments of off-grid power supplies, using renewable or alternative energy sources for remote mobile stations will grow from fewer than 13,000 worldwide in 2012 to more than 84,000 in 2020 [9]. China Mobile currently has one of the world's largest deployments of green technologies to power its base stations (BSs), with 2,135 BSs powered by alternative energy in 2008 according to [10]. Among these, 1,615 BSs of these were powered by solar energy, 515 by solar and wind energy and 5 by other alternative sources. According to predictions, the yearly number of green BSs deployments worldwide will grow from 13,000 in 2012 to more than 84,000 by 2020 [11]. More than 390,000 green BSs are expected to be deployed globally over this period. Solar and wind-powered cellular base stations are likely to become more popular in Africa, South Asia (including rural India), South America, Latin America, and the Caribbean where off-grid base stations are mainly deployed due to lack of power grids, as well as insufficient amount of fuel [10].

Various performance evaluation metrics, applicable to wind power systems have been defined in [12], [13] and [14]. Loss of load probability (LOLP), Loss of load expectation (LOLE) and the effective load carrying capability (ELCC) are defined in [13] with regards to only wind farms that generate huge amounts of energy in the hundreds of MW range to supply large scale consumers. The concept of capacity value is defined in [13] as means of quantifying the contribution of generating units or technologies to securing demand. The authors in [13] described the approximate methodologies for determining capacity values of power systems and also proposed a computational method for a system with non-renewable power sources integrated with wind power. The necessity of appending storage systems to the generated wind energy has also been affirmed by these papers, but with the emphasis limited to large amounts of energy without concern for flexibility. The authors in [15] have also derived indices such as LOLE, expected energy not supplied (EENS) and energy index of reliability (EIR) to evaluate the probabilistic reliability of off-grid hybrid solar PV-wind power system for the rural electrification in Nepal. This is also concerned with large amount of energy that is uneconomical for deployment in vehicular networks environments.

Some research efforts have been directed towards providing suitable energy storage for wind power systems due to the erratic nature of wind power for improved reliability [16-18]. There is currently a growing interest in the reliability study of power systems especially for critical telecommunication systems [19] but more importantly for determining adequacy of wind power [13]. The modelling and analysis of harnessed wind energy from the intermittent wind speed for communication systems are found to differ largely from the conventional power systems [13]. Furthermore, the authors in [14] present the reliability and economic evaluation of small autonomous power systems (SAPS) containing only renewable energy sources. The authors derived some basic probabilistic indices that define the performance of renewable energy powered systems since the conventional power systems reliability indices that are based on deterministic criteria cannot be applied in a system that contains only renewable energy sources (RES). RES have a time varying capacity which depends on the local atmospheric conditions and therefore cannot be modelled as deterministic.

In order to ensure that an off grid RSU powered by a small standalone wind energy conversion systems (SSWECS) [20] is able to meet the QoS for communication traffic, the reliability of the RSU which depends on the availability of wind and communication energy demand must be assessed. The stochastic nature of wind power is the prime reason for the evaluation of reliability indices. To the best of authors' knowledge, reliability modelling and analysis of an off-grid wind powered RSU, where reliability indices have been redefined in the context of variable wind power and transient energy demand, have not been carried out. Moreover, developing generic methods of scaling down battery sizes to enhance the flexibility of deploying dispersed roadside vehicular systems have not been undertaken.

3. THE STUDIED SCENARIO

The studied scenario considers a single RSU from a set of RSUs typically spaced 1 km apart along a 3 lane motorway stretch, which is in line with the wireless access for vehicular environment (WAVE) standard [21], as shown in Figure 1. The vehicles generate packets that arrive at the RSU through a collision and contention free channel [22]. The RSU collates the packets for the Internet through the BS. In this paper, the RSUs are battery operated wind powered off-grid standalone entities, coupled directly with a 0.5 m (diameter) micro turbine which has cut in (V_{cut_in}) and cut off (V_{cut_off}) speeds of 3.5 m/s and 21 m/s [23], respectively. The hourly average wind speed samples are obtained for the years 2009 to 2013 from the UK air information resource (AIR) database provided by the Department for Environment Food and Rural Affairs [24] at Newton, Reading, UK. The selected site is in the same geographical location as that of the M4 motorway stretch where hourly vehicular densities [25] have been obtained, for our analysis. Moreover, real packet size measurements [26] have also been utilised for performance evaluation. The parameters for the vehicular data generation, RSU operation and wind turbine are given in Table 1.

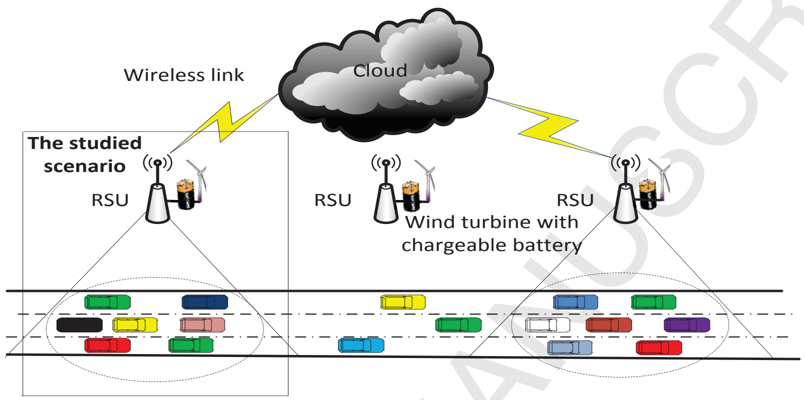

Figure 1: Wind powered RSUs in a motorway vehicular scenario.

Table 1: PARAMETERS FOR THE STUDIED SCENARIO.

Parameter	Notation	Value
RSU data rate	d_r	27 Mbps [2]
Vehicle data generation rate	d_t	320 kbps [27]
Vehicular density	M	3…36 [25]
Average packet size	P_s	867.4 bytes [26]
Packet arrival rate	λ	$d_t/(P_s \times 8)$
Packet departure rate	μ	$d_r/(P_s \times 8)$
RSU max. operational power	P_{max}	20 W [28]
RSU min. operational power	P_{Idle}	$P_{max}/1.3548$ [29]
Transmit Power	P_t^{RSU}	$P_{max} - P_{Idle} = 5.24$ W
Propeller length (diameter)	D	0.5 m [30]
Swept area	A	0.1963 m^2
Air density at 15^{0}C	ρ	1.225 kg/m^3 [31]
Coefficient of performance	C_p	0.45 [32]

Cut_in wind speed	V_{cut_in}	3.5 m/s [23]
Cut_off wind speed	V_{cut_off}	21 m/s [23]

4. WIND ENERGY MODEL

In order to develop a model for the harnessed wind energy from a micro-turbine, a detailed analysis of wind energy has been carried out using the hourly average wind speed samples at the RSU site which were obtained from the UK air information resource (AIR) database [24] for a period of five years. The samples were used to obtain the hourly probability distribution of wind speed which was found to follow Weibull distribution. Several authors have concluded that Weibull distribution is an acceptable instantaneous wind speed model [33], [34], [35]. The Weibull probability density function (pdf) is given as

$$f_v(v) = \frac{\beta}{\alpha}\left(\frac{v}{\alpha}\right)^{\beta-1} e^{-\left(\frac{v}{\alpha}\right)^{\beta}} \qquad v \geq 0 \tag{1}$$

where v is the instantaneous wind speed in m/s, α is the scale parameter in m/s, β is the unit-less shape parameter. The micro turbine parameters are shown in Table 1.

The mean and variance of Weibull distributed wind speed can be expressed as [36]

$$v_{mean} = \alpha\Gamma\left(1 + \frac{1}{\beta}\right) \tag{2}$$

and

$$v_{var} = \alpha^2\left[\Gamma\left(1 + \frac{2}{\beta}\right) - \left[\Gamma\left(1 + \frac{1}{\beta}\right)\right]^2\right] \tag{3}$$

where $\Gamma(x)$ denotes Gamma function of x. The mean and variance of wind speed at each hour can be determined from the obtained wind data of 5 years. With the mean and variance of wind speed, the Weibull parameters α and β are computed for each hour using (2) and (3). Table 2 shows the hourly wind speed parameters which are needed to be able to generate wind speed data at each hour of the day throughout the thesis. Figure 2 shows the wind speed pdf and its Weibull fit.

Table 2. WEIBULL PARAMETERS OF INSTANTANEOUS WIND SPEED.

Hour	Calculated Scale α (m/s)	Calculated Shape β	Average wind speed $\bar{v}$ (m/s) [24]

0	5.7	2.0	6.46
1	5.6	1.9	6.50
2	5.7	1.9	6.59
3	5.7	1.9	6.66
4	5.7	1.9	6.73
5	5.6	1.8	6.79
6	5.6	1.8	6.81
7	5.7	1.9	6.82
8	5.8	1.9	6.94
9	6.0	1.9	6.95
10	6.2	2.0	7.07
11	6.4	2.1	7.20
12	6.2	2.0	7.24
13	6.6	2.2	7.29
14	6.6	2.2	7.28
15	6.6	2.3	7.17
16	6.5	2.3	7.05
17	6.4	2.3	7.02
18	6.4	2.3	6.92
19	6.3	2.2	6.88
20	6.2	2.2	6.87
21	6.2	2.2	6.86
22	6.1	2.1	6.79
23	6.0	2.0	6.73

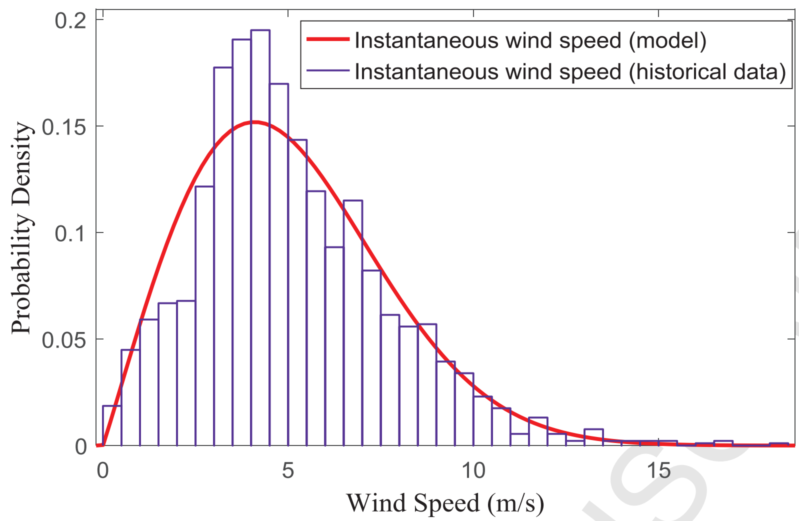

Figure 2: Model validation of instantaneous wind speed.

The instantaneous power harnessed from the wind can be expressed as

$$P_w = \frac{1}{2} C_p \rho A v^3 \tag{4}$$

where ρ is the air density (in kg/m^3); A is the turbine cross-sectional-area (in m^2), v is the wind speed normal to A (in m/s); and C_p is the coefficient of performance of the wind turbine, which accounts for the decrease in the actual power harnessed from the wind due to several factors such as rotor and blade design that lead to frictional and equipment losses.

Since the wind power is proportional to the third power of the wind speed as given in (4), the pdf of instantaneous power (P_w) which also follows Weibull distribution [37] is given as

$$f_P(x) = \frac{\beta}{3c_t\alpha^3}\left(\frac{x}{c_t\alpha^3}\right)^{(\beta/3)-1} e^{-\left(\frac{x}{c_t\alpha^3}\right)^{\beta/3}} \qquad x \geq 0 \tag{5}$$

where $c_t = A\rho C_p/2$, α and β are the wind speed scale and shape parameters, respectively. By comparing (5) with (1), the wind power pdf can be re-expressed in terms of wind power scale and shape parameters (α' and β') as

$$f_P(x) = \frac{\beta'}{\alpha'}\left(\frac{x}{\alpha'}\right)^{\beta'-1} e^{-\left(\frac{x}{\alpha'}\right)^{\beta'}} \qquad x \geq 0 \tag{6}$$

where $\alpha' = \frac{1}{2} A\rho C_p \alpha^3$; $\quad \beta' = \frac{\beta}{3}$.

The mean and variance of Weibull distributed power can also be expressed in terms of α' and β' [36] as

$$P_{w_{mean}} = \alpha' \Gamma\left(1 + \frac{1}{\beta'}\right) \tag{7}$$

and

$$P_{w_{var}} = \alpha'^2 \left[\Gamma\left(1 + \frac{2}{\beta'}\right) - \left[\Gamma\left(1 + \frac{1}{\beta'}\right)\right]^2\right] \tag{8}$$

Figure 3 shows both the simulated and modelled (Weibull distributed) wind power while the average hourly wind energy is shown in Figure 4. It is evident from Figure 4 that the hourly average wind power is peak at hours 13.00 and 14.00 due to the prevalent high wind speed at such times.

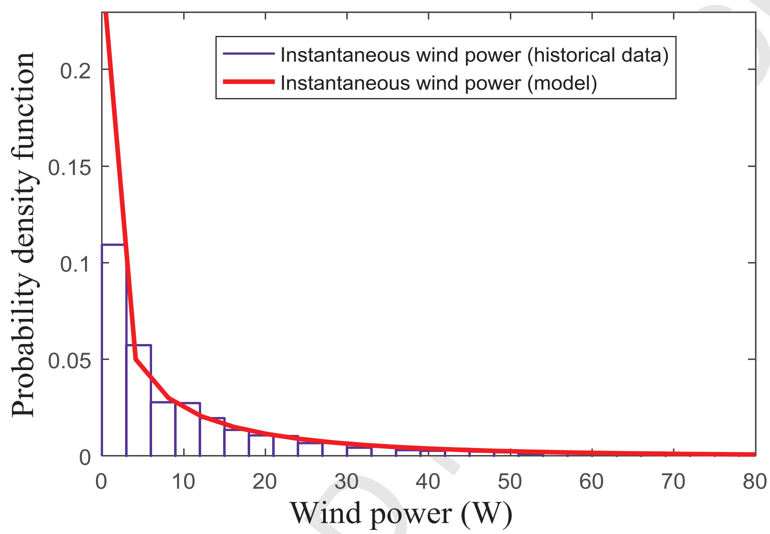

Figure 3: Model validation of instantaneous wind power.

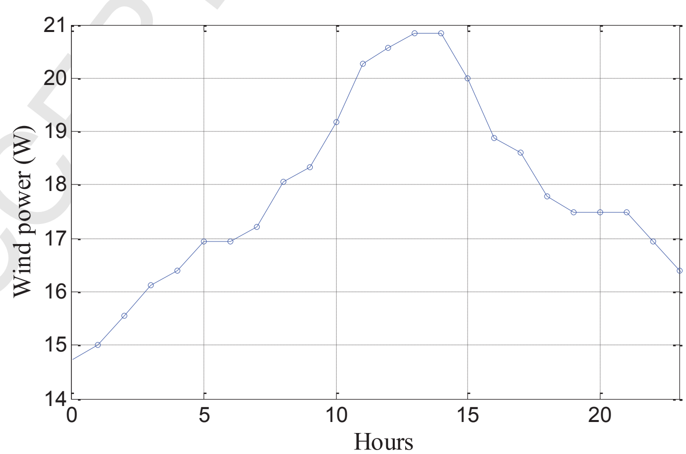

Figure 4: Hourly average wind energy.

5. Load Model of the RSU

The instantaneous power consumption of the RSU comprises of (a) the transmission energy per unit time which is dependent upon the varying data traffic corresponding to the vehicular density (M) and (b) the fixed power consumed by the RSU circuitry which is the minimum operational energy per unit time (P_{Idle}). Since most APs/RSUs usually have a separate transmitter circuit for the ease of implementing energy efficient transmission, the receiving and listening power consumptions belong to the fixed power aspect of the devices. A typical hourly vehicular flow and densities obtained from M4 motorway (UK) which lies within the same geographical location where the wind data were taken are shown in Figure 5. The transmission energy consumption by the RSU follows a Normal distribution with mean (μ) and standard deviation (σ) which vary hourly according to the vehicular density. This is because the transmission energy consumption by the RSU equals the traffic load or energy demand which directly depends on the product of traffic density and energy per bit. Packet arrivals are Poisson distributed, however energy per bit is evaluated over a very short time period and is approximated as Gaussian random variable. Gaussian distribution is an excellent approximation of Poisson distribution when the total number of events becomes sufficiently large [38].

Since the operational energy per unit time (P_{Idle}) is fixed, the probability density function of the energy consumption model can be expressed as

$$f(P_L) = \frac{1}{\sigma\sqrt{2\pi}} exp\left(-\frac{((P_L - P_{Idle}) - \mu)^2}{2\sigma^2}\right) \tag{9}$$

where the random variable P_L denotes the total energy consumption of the RSU per unit time. The parameters μ and σ represent the mean and standard deviation of the transmission energy consumption. Figure 6 shows the hourly average energy consumption by the RSU, which represents the summation of traffic energy demand and the fixed operational energy consumption of the RSU at each hour.

.

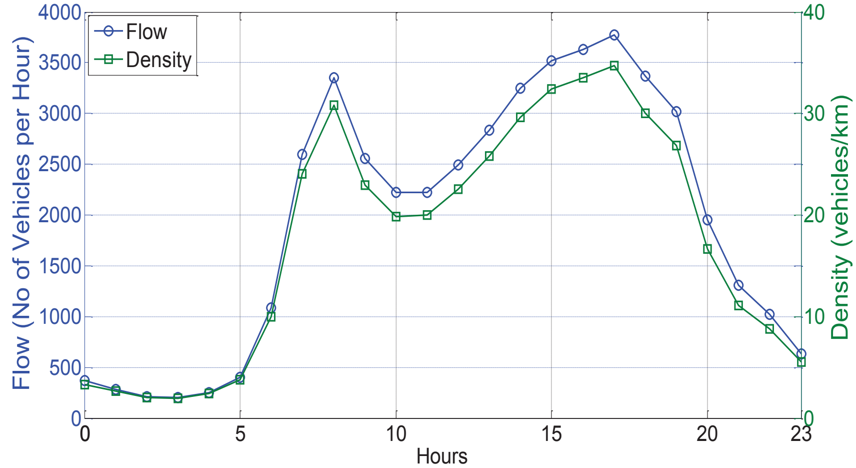

Figure 5: Hourly vehicular flow and density.

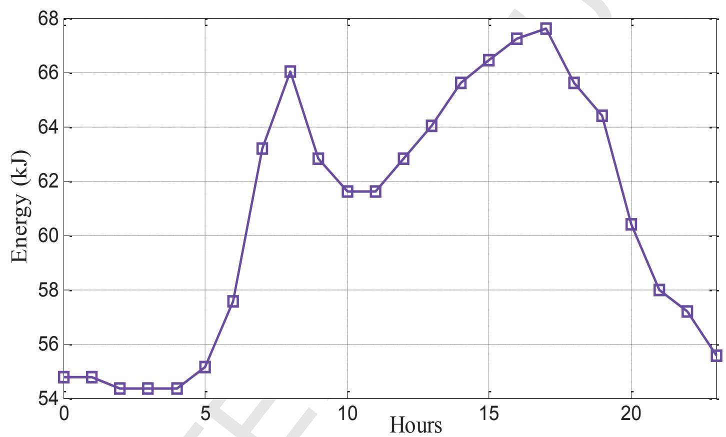

Figure 6: Hourly average energy consumption by an RSU.

6. RSU Reliability Modelling and Analysis

Reliability indices are used conventionally to analyse fault tolerance of automated systems. The concept of fault occurrence in automated systems is here applied to the off-grid RSUs in the context of the availability of wind power. Reliability analysis is crucial to ascertaining the communication feasibility of an off-grid RSU considering the stochastic nature of intermittent wind speed and hence the harnessed wind power. A number of related reliability indices are therefore redefined in this section.

Following on with the probabilistic models of load and wind power obtained in Chapter 3, the reliability analysis of the RSU is now considered here. To obtain the hourly outage of the RSU (failure due to insufficient wind energy), the hourly simulated wind and load energies for a period of 5 years which is equivalent to $I = 5 \times 365 = 1825$ days are compared pair-wise [14] as

$$Outage_t = \sum_{i=1}^{I} N(E_{Wti}, E_{Lti}) \quad (10)$$

where

$$N(E_{Wti}, E_{Lti}) = \begin{cases} 1 & if \ \ E_{Wti} < E_{Lti} \\ 0 & otherwise \end{cases}$$

where I represents the total number of days. The outage is assigned a value of 1 for an hour t on day i if the generated wind energy sample value (E_{Wti}) is less than the corresponding load energy sample value (E_{Lti}), and 0 otherwise. The loss of load probability (LOLP) [39] in our scenario in the present context can be redefined as

$$L_{lpt} = \frac{Outage_t}{I} \quad (11)$$

where L_{lpt} denotes loss of load probability at hour t. The expected loss of load over a specific time period represents another reliability index called loss of load expectation ($LOLE$). This is the average number of hours for which the load is expected to exceed the available capacity [14] and can be expressed in the present case as

$$L_{le} = \frac{1}{y} \sum_{t=1}^{T} (Outage_t) \quad (12)$$

where L_{le} represents loss of load expectation, y the total number of years and T the total number of hours in a day ($T = 24$). It signifies the average number of outage hours in a year.

To investigate the unmet capacity in the duration of study, the loss of energy expectation (LOEE) is determined. This is the expected energy in (kWh) that will not be supplied when the load exceeds the available generation, and can be derived from the hourly unmet demand in (10) as follows:

The unmet demand (U_{dti}) is the amount of energy deficit at any hour t over the total number of days ($I = y \times 365$) and can be expressed as

$$U_{dti} = \begin{cases} E_{Lti} - E_{Wti} & if \ E_{Lti} > E_{Wti} \\ 0 & otherwise \end{cases} \quad (13)$$

The loss of energy expectation (LOEE) denoted by L_{ee} is the total energy not met in a year and can be obtained as yearly average for y years case study as

$$L_{ee} = \frac{1}{y}\sum_{t=1}^{T}\{\sum_{i=1}^{I}(U_{dti})\} \qquad (14)$$

The EDNS which is the expected demand not served in an hour of the day (averaged over the 24 hours) can be obtained from the product of the state probability and the unmet demand for the hour as

$$E_{nst} = L_{lpt}\frac{1}{I}\sum_{i=1}^{I}(U_{dti}) \qquad (15)$$

The average EDNS over a 24 hour period can be expressed as

$$E_{ns} \quad = \frac{1}{T}\sum_{t=1}^{T} E_{nst} \qquad (16)$$

The EDNS in hour t is denoted by E_{nst}, while the average EDNS is denoted by E_{ns}. The energy index of reliability, E_{ir} [14] indicates the energy throughput of an RSU. It is the fraction of the expected load served to the total demand as applied to our study scenario:

$$E_{ir} = 1 - \frac{L_{ee}}{E_0} \qquad (17)$$

where E_0 is the energy demand of the RSU over the whole year. The energy index of unavailability, E_{iu}, which is the complement of EIR, can be expressed as

$$E_{iu} = \frac{L_{ee}}{E_0} \qquad (18)$$

The definitions of the various reliability indices used in this section are summarised in Table 3.

Table 3. DEFINITIONS OF RELIABILITY INDICES.

Reliability Index	**Definition**
$Outage_t$	The number of times wind power is less than load in a given hour t.
$LOLP_t$	Loss of load probability at hour t is the probability of wind power being less than load for the hour.
$LOLE$	Loss of load expectation is the number of times there is an outage in a year.
$LOEE$	Loss of energy expectation is the amount of energy not

	supplied/met in a year.
$EDNS_t$	Expected demand not served in an hour t is the product of state probability and the unmet demand for the hour.
EIR	Energy index of reliability is the proportion of energy requested that has been met.
EIU	Energy index of unavailability is the proportion of energy requested that has not been met.
FOR	Forced outage rate is the proportion of average outage time.

7. Analytic Models for LOLP, LOLE, LOEE, EDNS, MTBF, MTTR and FOR

The quantities of interest in Table 3 rely mainly on determining the probability that the load power is greater than the available wind power. Hence, the analytic models of the above reliability indices can be obtained from the probability density functions of wind energy and load. The instantaneous transmission energy consumption by the RSU follows a Normal distribution with mean (μ) and standard deviation (σ) according to the vehicular density as explained in Section 5. The instantaneous wind power follows Weibull distribution as discussed in Section IV. The pdfs of wind power and the RSU power demand (load) can be expressed respectively as

$$w(x) = \frac{\beta}{\alpha}\left(\frac{x}{\alpha}\right)^{\beta-1} e^{-\left(\frac{x}{\alpha}\right)^{\beta}} \tag{19}$$

and

$$l(y) = \frac{1}{\sigma\sqrt{2\pi}} e^{-\frac{\left((y-P_{Idle})-\mu\right)^2}{2\sigma^2}} \tag{20}$$

The L_{lpt} which represents the probability of failure, i.e., the probability that wind power is less than or equal to load can be expressed as

$$L_{lpt} = Prob\big(w(x) \leq l(y)\big) \tag{21}$$

Hence,

$$L_{lpt} = \int_{P_{Idle(t)}}^{P_{max(t)}} \left\{\int_0^y w_t(x)dx\right\} l_t(y)dy \tag{22}$$

where $w_t(x) = \frac{\beta_t}{\alpha_t}\left(\frac{x}{\alpha_t}\right)^{\beta_t-1} e^{-\left(\frac{x}{\alpha_t}\right)^{\beta_t}}$; $l_t(y) = \frac{1}{\sigma_t\sqrt{2\pi}} e^{-\frac{\left((y-P_{Idle})-\mu_t\right)^2}{2\sigma_t^2}}$ and P_{max} is maximum power demand (load). Substituting (19) and (20) in (21), (21) becomes

$$L_{lpt} = \int_{P_{Idle}}^{P_{max(t)}} \left\{ \int_0^y \frac{\beta_t}{\alpha_t} \left(\frac{x}{\alpha_t}\right)^{\beta_t - 1} e^{-\left(\frac{x}{\alpha_t}\right)^{\beta_t}} dx \right\} \frac{1}{\sigma_t\sqrt{2\pi}} e^{-\frac{\left((y-P_{Idle})-\mu_t\right)^2}{2\sigma_t^2}} dy \quad (23)$$

Integrating the integrand in bracket according to [40], (23) becomes

$$L_{lpt} = \int_{P_{Idle}}^{P_{max}(t)} (1 - e^{-\left(\frac{y}{\alpha_t}\right)^{\beta_t}}) \frac{1}{\sigma_t\sqrt{2\pi}} e^{-\frac{\left((y-P_{Idle})-\mu_t\right)^2}{2\sigma_t^2}} dy$$

Since solving the above integral is not possible analytically, if we are interested in the worst case hourly failure probability (L_{lpt}), then this occurs at $y = P_{max}$ in which case $y = P_{max}$ and $l_t(y) = 1$.

Hence,

$$L_{lpt} = 1 - e^{-\left(\frac{P_{max}}{\alpha_t'}\right)^{\beta_t'}} \quad (24)$$

$LOLE$ denoted by L_{le} can be expressed analytically in terms of L_{lpt} obtained in (6.15) as

$$L_{le} = \frac{1}{y} \sum_{t=1}^{T} \left(L_{lpt} \cdot I\right) \quad (25)$$

Where I represents the total number of days.

Similarly, the model for the LOEE, which represents the average unmet demand in a year, can be obtained as the product of failure probability and the total energy demand in a year as

$$L_{ee} = E_0 \frac{1}{T} \sum_{t=1}^{T} L_{lpt} \quad (26)$$

where L_{ee} denotes LOEE and E_0 is the total load demand in a year.

$EDNS_t$, the unmet energy in an hour, can also be expressed analytically as

$$E_{nst} = L_{ee_t} . L_{lpt} \quad (27)$$

where E_{nst} represents $EDNS_t$ and $L_{eet} = \frac{1}{I} \sum_{i=1}^{I} U_{dti}$.

The unavailability of sufficient wind power causes the RSU to fail. It remains non-operative until the available wind power becomes higher than the load energy. The corresponding down time duration is represented as time to recover (TTR). Similarly, the up time duration during which the RSU remains operative (till the RSU fails) is represented as time before failure (TBF), as shown in Figure 7.

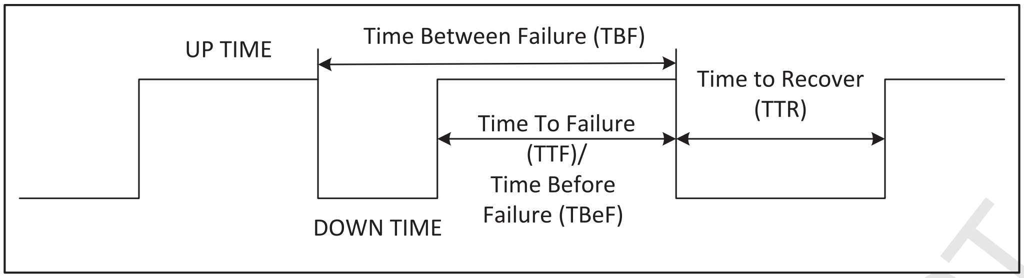

Figure 7: Reliability timing diagram of the RSU.

The average values of TTR and TBF over a certain duration can be defined as mean time to recover (MTTR) [41] and mean time before failure (MTBF) [41], which can be derived from the probability density functions of failure and recovery times obtained from wind and load energy samples. The reliability or survival rate function $R(t)$ of a Weibull distribution $f(t)$ [42] can be expressed as

$$R(t) = 1 - F(t) = e^{-\left(\frac{t}{\alpha}\right)^{\beta}} \tag{28}$$

where $F(t)$ is the CDF of $f(t)$. The hazard or failure rate $h(t)$ is the probability of failure at time Δt given that it has worked till time t. This can be written as

$$h(t) = \frac{f(t)}{R(t)} = \frac{\beta}{\alpha}\left(\frac{t}{\alpha}\right)^{\beta-1}. \tag{29}$$

The time before failure (T_{bf}) function is the reciprocal of the failure rate which is given as

$$T_{bf}(t) = \left(\frac{1}{h(t)}\right). \tag{30}$$

The mean time between failures (MTBF) can be obtained by taking expectation of $T_{bf}(t)$ over time t ranging from 0 to ∞.

The downtime pdf $D(t)$ can be expressed as the probability that the wind power is less than the load power for any given value of load power for the duration of time t. Therefore, it is the complement of the reliability function and is expressed as

$$D(t) = 1 - R(t) = F(t) \tag{31}$$

Time to repair denoted by T_{tr} can be expressed as

$$T_{tr}(t) = \frac{1}{D(t)} \tag{32}$$

The mean time to repair (MTTR) can be obtained by taking expectation of $T_{tr}(t)$ over time t to ∞. The forced outage rate (FOR) denoted by F_r can be expressed in terms of MTTR and MTBF [43] as

$$F_r = \frac{MTTR}{MTBF+MTTR} \tag{33}$$

8. Results and Discussions

The pdf of positive $P_w - P_L$ is shown in Figure 8 while Figure 9 shows the pdf of negative $P_w - P_L$. The energy deficit and surplus levels of the RSU have been obtained from the energy consumption and wind energy models. The hourly surplus/deficit energy is obtained by subtracting the hourly energy demand from hourly wind energy. The positive and the negative values obtained for 1825 hourly samples are used for the probability density plots in Figure 8 and Figure 9.

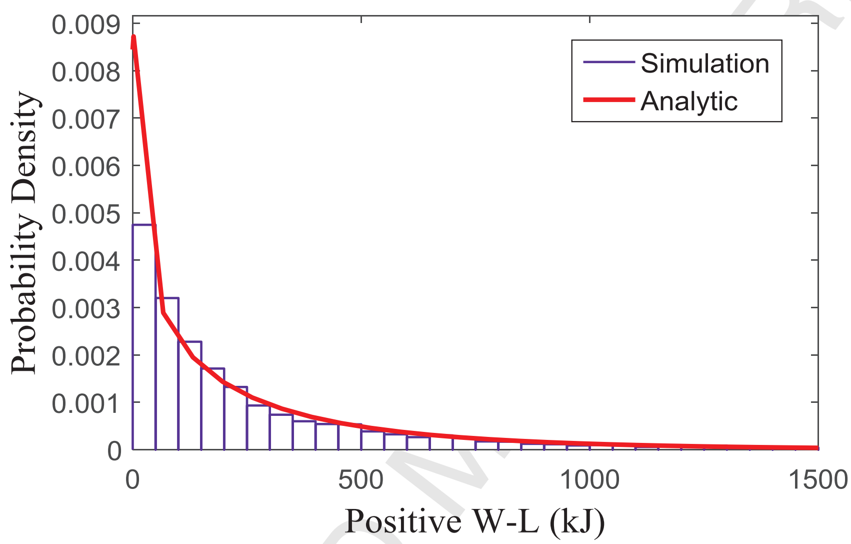

Figure 8: Probability density function of instantaneous (positive) $\boldsymbol{P_w - P_L}$.

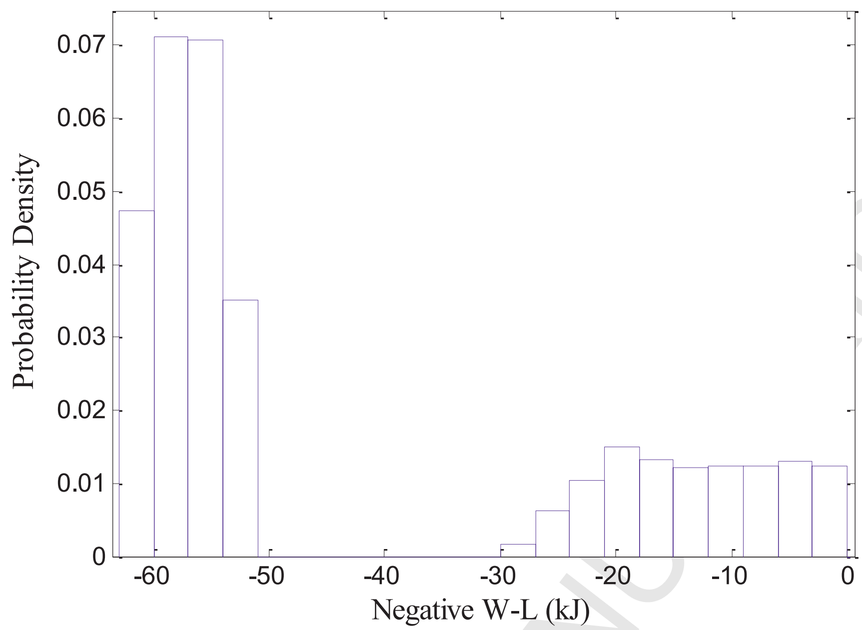

Figure 9: Probability density function of instantaneous (negative) $\boldsymbol{P_w - P_L}$.

It is clear from Figure 8 and Figure 9 that there are number of instances where the wind energy is insufficient to keep the RSU operational. The computation of surplus/deficit energy from a sample size of 43800 reveals 36.9% energy deficiency (negative $P_w - P_L$) and 63.1% energy surplus (positive $P_w - P_L$). As seen in Figure 9, deficits beyond -30 kJ (i.e. -50 kJ to -72 kJ) refer to the unavailability of wind energy due to very low (i.e. less than cut-in) wind speed. The deficit that occurs from the moment the wind speed attains the cut-in speed of 3.5 m/s and above is shown between -30 kJ and 0 kJ as the turbine now functions. There is no deficit between -30 kJ and -50 kJ as the minimum load energy which constitutes the deficit when the turbine has zero output is 54 kJ. The high percentage surplus energy realised can be stored to meet the incurred deficit.

With the surplus energy being almost twice the deficit energy, the additional surplus energy after meeting the deficit via battery can be disregarded as it cannot be injected back into the grid (RSU is off-grid standalone). This is to prevent the continuous build-up of surplus energy and limit the size of battery for the standalone RSU. Moreover, determining the required battery size for a given communication demand is crucial for the ease of deployment. Thus the battery with minimum capacity should be able to cater for the maximum deficit at any point in time during the whole day. The instantaneous cumulative energy level can be obtained as

$$C = C' + (E_w - E_L) \tag{34}$$

where C denotes the current energy level and C' denotes the previous energy level in the battery, and is set to an initial value of 0 kJ. E_W and E_L represent the generated instantaneous wind (i.e. available) and load (i.e. demand) energies, respectively. To determine the maximum discharge level (i.e. deficit), we disregard the surplus energy by placing a ceiling as $C = 0$. The resulting maximum discharge level of -637 kJ obtained for the studied scenario requires a maximum battery of size 29.4 Ah (considering a 12 V deep cycle battery with a 50% depth of discharge (DOD) [44]). However to determine the minimum battery size which facilitates a certain level of reliability and QoS, the cumulative discharge level needs to be converted into the probabilistic domain by obtaining cumulative probability plot for the discharge behaviour.

Having determined the battery sizes for 96% and 99.9% availabilities as 7.9 Ah and 22.7 Ah respectively, the performance of the RSU is evaluated with respect to key reliability indices for the three cases: I) No battery, II) 7.9 Ah battery, and III) 22.7 Ah battery. The respective analytic models are verified with simulation. The battery sizes of 7.9 Ah and 22.7 Ah yield 96% and 99.9% availabilities, respectively.

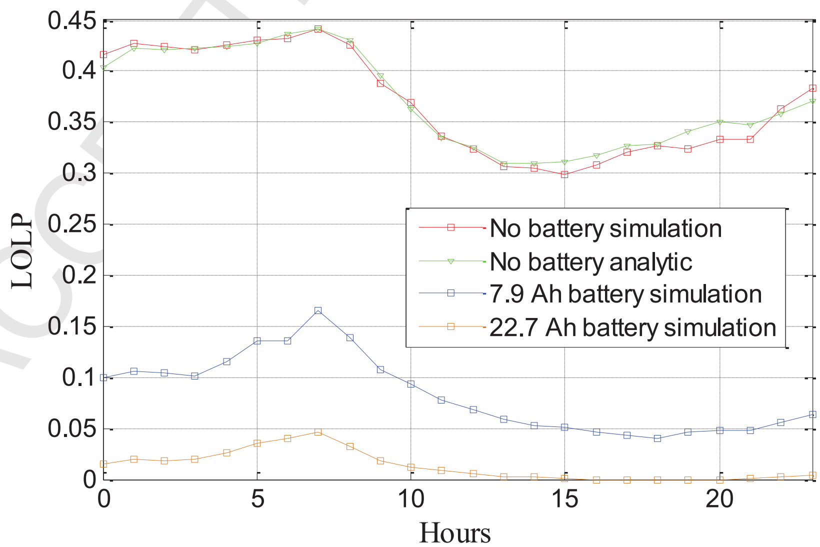

Figure 10: LOLP of the RSU with and without battery.

Figure 10 shows the hourly probability of failure (LOLP) (both simulation and analytic results) for the three cases: I) No battery, II) 7.9 Ah battery and III) 22.7 Ah battery against the hours of the day. As expected, in the case of no battery, the LOLP is very high (i.e. up to 0.44) at some hours of the day. This is due to the relatively low wind energies (see Figure 4) compared to the load demands (Figure 6) at those hours, thus, necessitating the need for integrating a battery. During the midday the load demand increases, however the wind energy increases substantially resulting in a much lower LOLP even without a battery. The LOLP for the RSU with no battery remains relatively high, ranging between 0.30 and 0.44. A 7.9 Ah battery enabling 96% availability lowers the LOLP to a range below 0.1 for most hours of the day while 22.7 Ah battery which presents 99.9% availability keeps the LOLP at 0 for most hours of the day.

While the hourly LOLP represents the shortage probability, the EDNS signifies the amount of shortage. Thus the hourly EDNS (Figure 11) exhibits a similar trend as that of hourly LOLP (Figure 10). The hourly EDNS in the case with no battery has a peak of 9.35 kJ at 0800 hrs with a minimum of 4.12 kJ at 1600 hrs. The EDNS for the cases with batteries are significantly low as expected. For example, the 7.9 Ah battery lowered the EDNS to a maximum of 1.28 kJ while 22.7 Ah battery maintained EDNS around 0 kJ for most of the day.

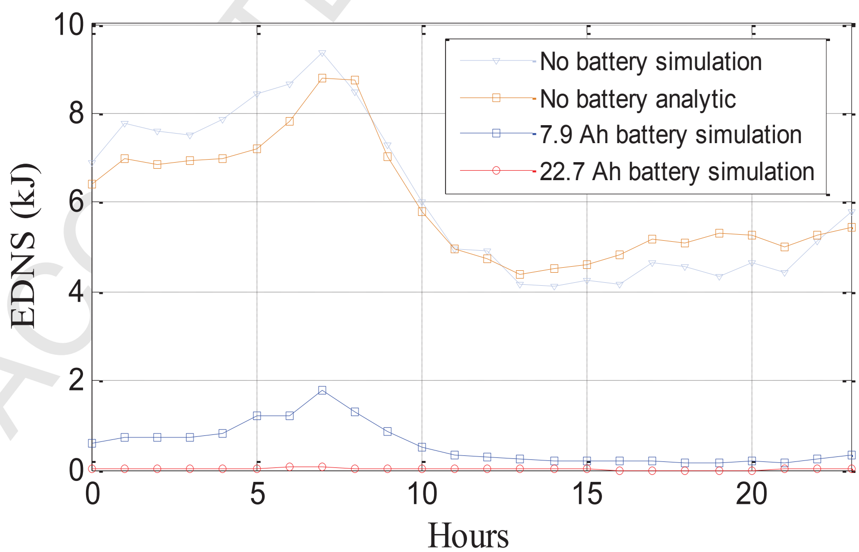

Figure 11. EDNS with and without battery.

To determine FOR, the MTBF and MTTR are obtained by taking samples of uptimes and downtimes of the RSU. These are used to obtain distributions of time between failures and time to recover, as shown in Figure 12 and Figure 13 respectively. Figure 12 shows the survivor function of the time between failures for all the four cases. The survivor function, also known as a survival function or reliability function, is a property of any random variable that maps a set of events (in this case failure of an RSU), onto time. It indicates the probability of a system or unit surviving until a given time, i.e. time before failure in this application. The various time limits (in hours) the RSU can function reliably or survive is shown against the probability of reliability as survivor function. The RSU with no battery (i.e. case I) only lasts a maximum of 20 hours before a failure. Case II (with 7.9 Ah battery) can provide continuous operation of up to 500 hours while case III (with 22.7 Ah battery) achieves a maximum of 35,000 hours of uninterrupted service. As expected in all reliability indices, the survivor function approaches zero as age (mean time before failure in this case) increases without bound.

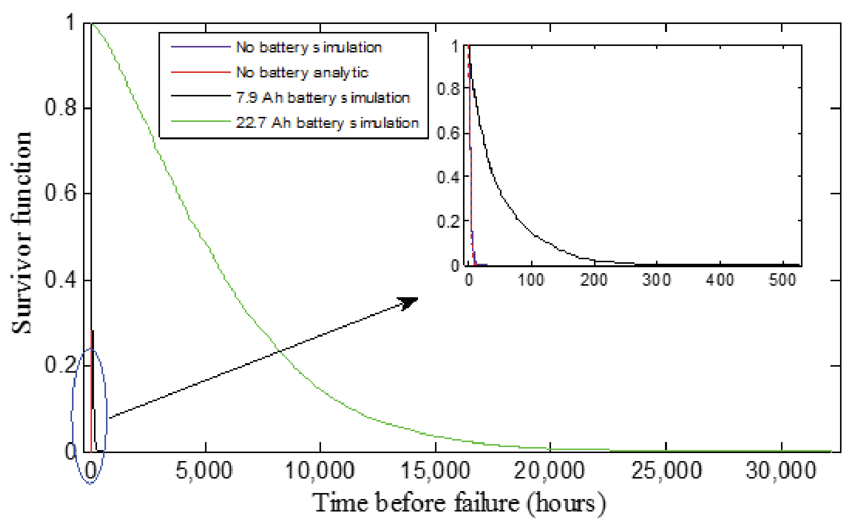

Figure 12: Time before failure (TBF) with and without battery.

The simulation result of the time to recover, as in Figure 13, shows that recovery time for all cases (with and without batteries) is primarily between 1 to 2 hours, reaching up to 11 hours rarely. Although all the cases exhibit very similar recovery times, inclusion of larger battery moves the curves in Figure 13 up, i.e., the probability of the system recovering within say 4 hours is a higher probability (area under curve) if a larger battery is used.

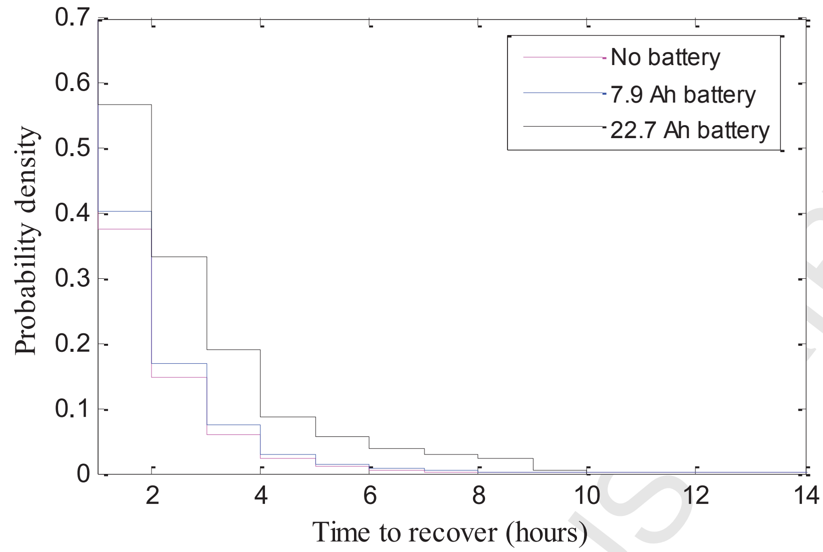

Figure 13: Time to recover (TTR) pdf with and without battery.

The overall reliability of the RSU is analysed using the LOLE, EIR, EIU and FOR as shown in Figure 14. The LOLE without a battery is 36.9% which corresponds to the percentage of energy deficit. This is expected since the loss of load is caused by energy deficiency. Hence the probability of such energy deficiency is equivalent to the LOLE. A 7.9 Ah battery brings the LOLE down to 8.3% while 22.7 Ah achieves a very low LOLE of 1.4%. The EIR without battery subsequently has lower value (i.e. 72%) compared to the 89.9% with a 7.9 Ah battery and even higher (99%) with a 22.7 Ah battery. The unavailability index (EIU) attains 28.1% with no battery while the cases of 7.9 Ah and 22.7 Ah battery-equipped RSU are limited to 10% and 1.3% $\boldsymbol{EIU}$, respectively. These are all due to the fact that less RSU failure or outage occurs with increased energy supply from wind and battery of relatively bigger sizes.

The MTBF predicts the average uptime whereas the MTTR predicts the average duration of outages. The MTBF and MTTR are used to determine the FOR in (33). As shown in Figure 14 the integration of a battery with the RSU significantly improves the MTBF, whereas the improvement in MTTR is marginal as recovery is independent of a battery size. As expected, FOR is highest for the no battery case. Battery addition reduces the FOR from 27% to 2.1% and 0.02% respectively with 7.9 Ah and 22.7 batteries. These are once again due to the fact that less RSU failure or outage occurs with increased energy supply from wind and relatively bigger size battery. The MTBF is hence improved, leading to a reduced forced outage rate.

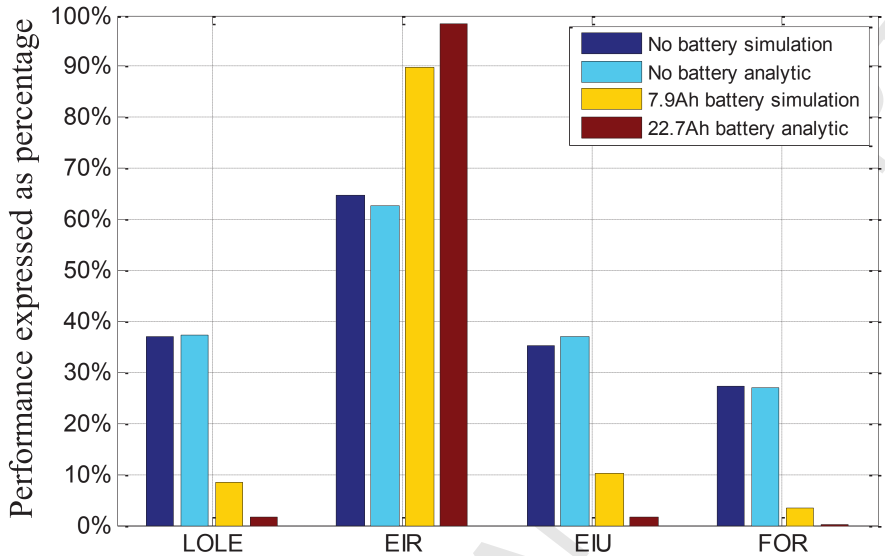

Figure 14: Overall performance of the RSU.

Finally, the QoS of the RSU is evaluated in terms of packet dropping (or blocking) probability, average packet delay and throughput while considering the RSU as a queue with an infinite buffer. The real channel impairments are ignored in this analysis for the purpose of investigating the performance of the RSU in the context of its energy supply only. The assumption of RSU having infinite buffer is not far-fetched as modern access points can be equipped with large memory such as embedded multimedia card (EMMC) [45]. Since the RSU has an infinite buffer, the packets are only lost (blocked) due to the unavailability of the RSU. Hence, the LOLP is the packet dropping (blocking) probability. Having already obtained the packet dropping probability (i.e. LOLP), we now determine the average packet delay at the RSU.

A typical grid connected RSU serves all packets at the maximum data rate (d_r). However, the RSU in our case drops all the arriving packets during its down time (when unavailable). To determine the throughput and the average packet delay for the successfully transmitted packets, the RSU is modelled as an *M/M/1* queue [46] where the first *M* represents the Poisson arrival of the packets from the vehicles, second *M* refers to the service rate and 1 denotes the number of server (i.e. RSU transmitter). Thus, the hourly average packet delay W_t can be obtained from the response time expression of an *M/M/1* queue as

$$W_t = \frac{1}{\mu - M\lambda_t(1 - LOLP_t)}. \tag{35}$$

Here M refers to the hourly density of vehicles. Figure 15 shows the average packet delay against the hours for all the four cases. The values of M, the arrival rate (λ) and the service rate (μ) used in this computation are obtained from the vehicular traffic profile at M4. The average packet delay is relatively low in all the cases with the values ranging between 0.26 ms and 0.45 ms. The average packet delay is lowest in case I due to the less number of packets awaiting service in the buffer after a significant packet loss arising from high $LOLP_t$. The reduced $LOLP_t$ in cases II and III resulted into a slightly higher average packet delay as the buffer now has an increased number of waiting packets to be served by the RSU.

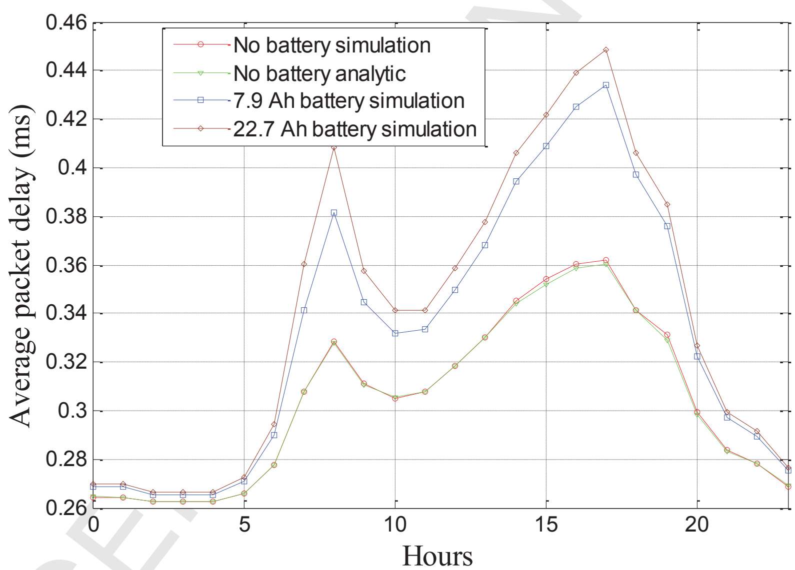

Figure 15: Average packet delay of the RSU.

Similarly, the hourly throughput (X_t) of the RSU can be obtained as

$$X_t = M\lambda_t(1 - LOLP_t) \tag{36}$$

As shown in Figure 16, the average throughput of the RSU varies inversely with the $LOLP_t$ as expected. The case I with no battery which has the highest $LOLP_t$ portrays the lowest throughput at all time. This is evident from the fact that many packets were dropped by the RSU during its periods of unavailability. The two cases with different battery sizes show improved throughput with the 22.7 Ah battery having the highest (1500 packets/s). The two peak values in both Figure 15 and Figure 16 at hours 8.00 and 17.00 are in conformity with the peak vehicular flow and density at such busy hours of the day.

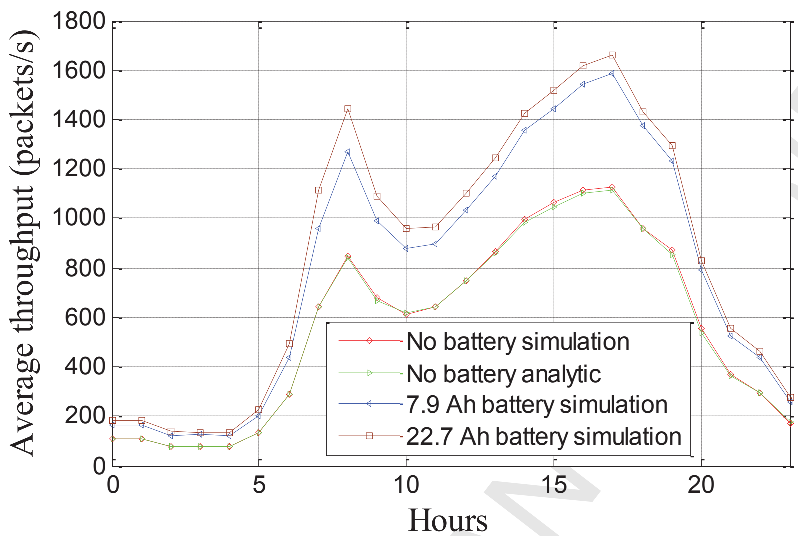

Figure 16. Average throughput of the RSU.

COMPARISON WITH OTHER WINDY AND NON-WINDY LOCATIONS

The hourly wind speed data for different US cities (San Francisco, Berkeley, Boston and Galveston) for a period of 5 years [47] were obtained and the instantaneous wind energies were generated at each location through the wind model. To represent vehicular traffic of these cities, an hourly vehicular densities from I-80 inter-state expressway [48] were obtained and the instantaneous load energies were generated through the load model.

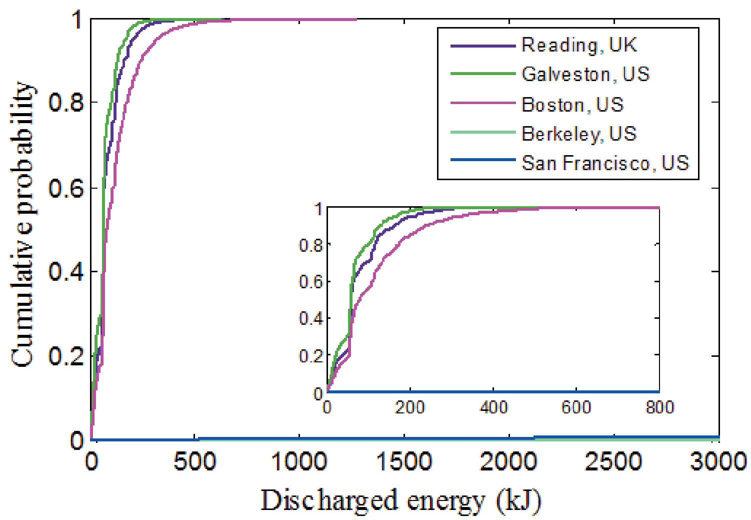

Figure 17: Comparative cumulative probability of discharged energy.

Figure 17 compares the cumulative deficits of the various cities investigated. The x-axis represents the cumulative deficit while y-axis is the probability that the cumulative deficit is less than say 500 kJ. From the computation of total surplus/deficit energy based on the source data, it is found that locations such as San Francisco and Berkeley in the US do not have sufficient wind speed and the yearly average deficit indicates acute wind energy shortages i.e. 27 kWh and 47 kWh, respectively where a single RSU is considered. Therefore, integrating an energy-storage (e.g. fast rechargeable battery) will be meaningless since the battery will be unable to recharge due to the insufficient wind energy in such locations. However, windy locations in the US such as seaside Galveston and I-80 stretch near Boston are found to have on average yearly surplus wind energy i.e. 380 kWh and 195 kWh while the main city of study interest (Reading, UK) has enough yearly wind energy i.e. 412 kWh average yearly surplus.

As discussed before, the continuous deficit of wind energy results in very large cumulative discharged energy in non-windy locations such as San Francisco and Berkeley (see Figure 17). Therefore, any battery size would be insufficient (given our RSU and wind turbine parameters, and wind speeds) in these locations due to the lack of wind energy required for recharging. However, significantly lower battery sizes are required in windy locations like Reading (UK) and Galveston compared to Boston. Considering a 12 V deep cycle battery with a 50% *depth of discharge* (DOD) [44], a battery size of 28.8 Ah is required in Galveston compared to 59 Ah in Boston to completely eradicate outage while in Reading, UK, a battery size of 29.4 Ah is needed. The respective maximum battery sizes for the various cities were obtained from their maximum cumulative discharged energies which are 637 kJ, 623 kJ, 1277 kJ, 479100 kJ and 851095 kJ for Reading, Galveston, Boston, San Francisco and Berkeley respectively. The battery size in general can further be reduced if a certain percentage of outage is allowed. However, this requires further in depth analysis with the help of the discussed reliability indices.

9. CONCLUSIONS

In this paper, we carried out transient analyses of energy consumption of an RSU and harnessed wind energy from a micro-turbine for that RSU in a motorway vehicular environment. Subsequently we proposed corresponding analytic models. Furthermore, we proposed analytic model for obtaining the minimum battery size for achieving certain levels of reliability and Quality of Service (QoS). The main thrust of this work is to redefine and model usual reliability indices in the context of intermittent availability of wind power in vehicular communications. The transient models and the reliability analyses proposed in this paper are generic and can be used for any location, where the need for fast and standalone RSU deployment is of paramount importance.

Considering the M4 motorway vehicular environment as a study scenario, we evaluated the performance of a wind powered RSU in terms of reliability indices such as loss of load probability, expected demand not served, loss of load expectation, energy index of reliability and forced outage rate, and QoS parameters such as average packet delay and throughput. The forced outage rate of 27% with no battery was brought down to only 0.03% with a battery of size 22.7 Ah. Similarly, the loss of load probability was reduced to 0.009 (almost zero) with 22.7 Ah battery, compared to the case of no battery where the loss of load probability was 0.44 at some hours of the day. The results revealed that the RSU was able to achieve 90% and 99% reliabilities with 7.9 Ah and 22.7 Ah batteries, respectively. The achieved reliability is good compared to the industrial standard reliability (99.9% or 99.999%) which is maintained with adequate resource provisioning. Furthermore, the RSU achieved an acceptable average packet delay (between 0.26 ms and 0.45 ms) for all the cases studied and equally showed an improved throughput of up to 50% with the least battery size considered in the study.

Acknowledgement

The authors would like to acknowledge the support of the Engineering and Physical Sciences Research Council (EPSRC), UK for funding the INTelligent Energy awaRe NETworks (INTERNET) project under contract EP/H040536/1; and Petroleum Technology Trust Fund, Nigeria, for the Scholarship awarded to the first author to fund his PhD. All data are provided in full in the results section of this paper.

References

[1] E. Taylor, A. Humphrey, K. Pickering, and S. Tipping, "National Travel Survey 2011 Technical Report," *Prepares for UK Department for Transport,* 2012.

[2] W. Kumar, S. Bhattacharya, B. R. Qazi, and J. M. Elmirghani, "A vacation-based performance analysis of an energy-efficient motorway vehicular communication system," *Vehicular Technology, IEEE Transactions on,* vol. 63, pp. 1827-1842, 2014.

[3] D. J. Arent, A. Wise, and R. Gelman, "The status and prospects of renewable energy for combating global warming," *Energy Economics,* vol. 33, pp. 584-593, 2011.

[4] A. Muhtar, B. R. Qazi, S. Bhattacharya, and J. M. Elmirghani, "Greening vehicular networks with standalone wind powered RSUs: A performance case study," in *Communications (ICC), 2013 IEEE International Conference on*, 2013, pp. 4437-4442.

[5] P. Grant and S. Fletcher, "Mobile basestations: Reducing energy," *Engineering and Technology Magazine,* vol. 6, 2011.

[6] G. Auer, V. Giannini, C. Desset, I. Godor, P. Skillermark, M. Olsson, *et al.*, "How much energy is needed to run a wireless network?," *Wireless Communications, IEEE,* vol. 18, pp. 40-49, 2011.

[7] W. Feng, H. Alshaer, and J. M. Elmirghani, "Green information and communication technology: energy efficiency in a motorway model," *Communications, IET,* vol. 4, pp. 850-860, 2010.

[8] I. Humar, X. Ge, L. Xiang, M. Jo, M. Chen, and J. Zhang, "Rethinking energy efficiency models of cellular networks with embodied energy," *Network, IEEE,* vol. 25, pp. 40-49, 2011.

[9] *Off-Grid Power for Mobile Base Stations - Renewable and Alternative Energy Sources for Remote Mobile Telecommunications: Global Market Analysis and Forecasts*. Available: http://www.prnewswire.com/news-releases/off-grid-power-for-mobile-base-stations---renewable-and-alternative-energy-sources-for-remote-mobile-telecommunications-global-market-analysis-and-forecasts-188185711.html

[10] L.-C. Wang and S. Rangapillai, "A survey on green 5G cellular networks," in *Signal Processing and Communications (SPCOM), 2012 International Conference on*, 2012, pp. 1-5.

[11] J. Lorincz, I. Bule, and M. Kapov, "Performance Analyses of Renewable and Fuel Power Supply Systems for Different Base Station Sites," *Energies,* vol. 7, pp. 7816-7846, 2014.

[12] M. Shaaban and M. Usman, "Risk Assessment of Wind Generation Dispatch Using Monte Carlo Simulation," *International Journal of Smart Grid and Clean Energy,* vol. 2, pp. 258-263, 2013.

[13] A. Keane, M. Milligan, C. J. Dent, B. Hasche, C. D'Annunzio, K. Dragoon, *et al.*, "Capacity value of wind power," *IEEE Transactions on Power Systems,* vol. 26, pp. 564-572, 2011.

[14] P. S. Georgilakis and Y. A. Katsigiannis, "Reliability and economic evaluation of small autonomous power systems containing only renewable energy sources," *Renewable Energy,* vol. 34, pp. 65-70, 2009.

[15] N. Pradhan and N. R. Karki, "Probabilistic reliability evaluation of off-grid small hybrid solar PV-wind power system for the rural electrification in Nepal," in *North American Power Symposium (NAPS), 2012*, 2012, pp. 1-6.

[16] M.-S. Lu, C.-L. Chang, W.-J. Lee, and L. Wang, "Combining the wind power generation system with energy storage equipments," in *Industry Applications Society Annual Meeting, 2008. IAS'08. IEEE*, 2008, pp. 1-6.

[17] J. P. Barton and D. G. Infield, "Energy storage and its use with intermittent renewable energy," *Energy Conversion, IEEE Transactions on,* vol. 19, pp. 441-448, 2004.

[18] S. Teleke, M. E. Baran, A. Q. Huang, S. Bhattacharya, and L. Anderson, "Control strategies for battery energy storage for wind farm dispatching," *Energy Conversion, IEEE Transactions on,* vol. 24, pp. 725-732, 2009.

[19] D. G. Robinson, D. J. Arent, and L. Johnson, "Impact of distributed energy resources on the reliability of critical telecommunications facilities," in *Telecommunications Energy Conference, 2006. INTELEC'06. 28th Annual International*, 2006, pp. 1-7.

[20] R. Billinton, "Bagen. A sequential simulation method for the generating capacity adequacy evaluation of small stand-alone wind energy conversion systems," in *IEEE CCECE02 Proceedings*, 2002, pp. 72-77.

[21] R. Uzcategui and G. Acosta-Marum, "Wave: a tutorial," *Communications Magazine, IEEE,* vol. 47, pp. 126-133, 2009.

[22] W. Guo, L. Huang, L. Chen, H. Xu, and J. Xie, "An adaptive collision-free MAC protocol based on TDMA for inter-vehicular communication," in *Wireless Communications & Signal Processing (WCSP), 2012 International Conference on*, 2012, pp. 1-6.

[23] (2013). *Wind Turbine Curves: Wind Power Program*. Available: http://www.wind-power-program.com/turbine_characteristics.htm

[24] *Department for Environment Food and Rural Affairs*. Available: uk-air.defra.gov.uk/

[25] W. Kumar, S. Bhaacharya, B. R. Qazi, and J. M. H. Elmirghani, "An energy efficient double cluster head routing scheme for motorway vehicular networks," in *Communications (ICC), 2012 IEEE International Conference on*, 2012, pp. 141-146.

[26] C. Fraleigh, S. Moon, B. Lyles, C. Cotton, M. Khan, D. Moll*, et al.*, "Packet-level traffic measurements from the Sprint IP backbone," *Network, IEEE,* vol. 17, pp. 6-16, 2003.

[27] X. Wu, S. Wu, H. Sun, and L. Li, "Dynamic slot allocation multiple access protocol for wireless ATM networks," in *Communications, 1997. ICC'97 Montreal, Towards the Knowledge Millennium. 1997 IEEE International Conference on*, 1997, pp. 1560-1565.

[28] (2013). *ARUBA Networks "Aruba AP-85FX and AP-85LX Access Points"*. Available: http://www.mayflex.com/_assets/downloads/DS_AP85FXLX.pdf

[29] L. Haratcherev, M. Fiorito, and C. Balageas, "Low-power sleep mode and out-of-band wake-up for indoor access points," in *GLOBECOM Workshops, 2009 IEEE*, 2009, pp. 1-6.

[30] (2007, "Wren Micro-Turbine (datasheet)". *supplemented with the manuscript: Samrey Generators & Turbines Ltd.*

[31] G. M. Masters. (2004). *Renewable and Efficient Electric Power Systems (First Edition ed.)*.

[32] (2013). *Practical Action: Wind Energy Generation*. Available: http://practicalaction.org/docs/technical_information_service/wind_electricity_generation.pdf

[33] S. A. Akdağ and A. Dinler, "A new method to estimate Weibull parameters for wind energy applications," *Energy conversion and management,* vol. 50, pp. 1761-1766, 2009.

[34] A. N. Celik, "A statistical analysis of wind power density based on the Weibull and Rayleigh models at the southern region of Turkey," *Renewable Energy,* vol. 29, pp. 593-604, 2004.

[35] A. Altunkaynak, T. Erdik, İ. Dabanlı, and Z. Şen, "Theoretical derivation of wind power probability distribution function and applications," *Applied Energy,* vol. 92, pp. 809-814, 2012.

[36] H. Pham. (2006). *Handbook of Engineering Statistics*.

[37] D. Villanueva and A. Feijóo, "Wind power distributions: A review of their applications," *Renewable and Sustainable Energy Reviews,* vol. 14, pp. 1490-1495, 2010.

[38] J. H. Einmahl, "Poisson and Gaussian approximation of weighted local empirical processes," *Stochastic processes and their applications,* vol. 70, pp. 31-58, 1997.

[39] R. Allan and R. Billinton, "Probabilistic assessment of power systems," *Proceedings of the IEEE,* vol. 88, pp. 140-162, 2000.

[40] I. S. Gradshteyn and I. M. Ryzhik, *Table of integrals, series, and products*: Academic press, 2014.

[41] M. Krasich, "How to estimate and use MTTF/MTBF would the real MTBF please stand up?," in *Annual Reliability and Maintainability Symposium (RAMS)*, January 2009, pp. 353-359.

[42] M. Rausand and A. Høyland, *System reliability theory: models, statistical methods, and applications* vol. 396: John Wiley & Sons, 2004.

[43] C. Oggerino, *High availability network fundamentals*: Cisco Press, 2001.

[44] D. G. Photovoltaics and E. Storage, "IEEE Recommended Practice for Sizing Lead-Acid Batteries for Stand-Alone Photovoltaic (PV) Systems," 2007.

[45] Y. Choi, H. Jeong, and H. Kim, "Future evolution of memory subsystem in mobile applications," in *Memory Workshop (IMW), 2010 IEEE International*, 2010, pp. 1-2.

[46] J. F. S. D. Gross, J. M. Hompson, and C. M. Harris. *Fundamentals of Queueing Theory (4th ed.)*.

[47] *Windguru*. Available: http://www.windguru.cz/

[48] N. Wisitpongphan, F. Bai, P. Mudalige, V. Sadekar, and O. Tonguz, "Routing in sparse vehicular ad hoc wireless networks," *Selected Areas in Communications, IEEE Journal on,* vol. 25, pp. 1538-1556, 2007.